Simulating cement hydration using HYDCEM

Holmes, N., Kelliher, D. & Tyrer, M.

Simulating cement hydration using HYDCEM

Niall Holmes[1,*], Denis Kelliher[2] & Mark Tyrer[3]

[1]School of Civil & Structural Engineering, Dublin Institute of Technology, Dublin 1, Ireland

[2]School of Civil, Structural and Environmental Engineering, University College Cork, Cork. Ireland

[3]Centre for Research in the Built and Natural Environment, Coventry University, UK

Phone: +353 1 402 4039

Email: niall.holmes@tudublin.ie

*Corresponding Author

Abstract

HYDCEM is a new cement hydration model to simulate volumetric changes and predict phase assemblage, degree of hydration, heat release, compressive strength and chemical shrinkage over time for PC and limestone binders undergoing hydration for any w/c ratio and curing temperatures between 5 to 45^0C. While hydration models should never completely remove experimental analysis, they are an aid to better understand cement hydration and microstructure development by allowing users analyse different binders in a relatively short time. HYDCEM, written in MATLAB®, is aimed at complementing more sophisticated thermodynamic models giving users a reasonable prediction of hydration behaviour over time using user-customisable inputs. A number of functions based on up to date cement hydration behaviour from the literature are included along with user-changeable inputs such as the cement chemical (oxide) composition, cement phase densities, species molar mass, phase and product densities and heat of hydration enthalpies. HYDCEM uses this input to predict the cement phase and gypsum proportions, volume stoichiometries and dissolution and growth of hydration products from the silicates, aluminates and ferrites, including C-S-H, calcium hydroxide, hydrogarnet (if applicable), hydrotalcite, ettringite, monosulphate, hemicarbonate and monocarbonate of limestone is present. A number of comparisons with published experimental and thermodynamic model results and HYDCEM predictions are made to assess its accuracy and usefulness. Previous work has shown that HYDCEM can reasonably accurately predict phase assemblages in terms of volume change and behaviour for a range of cements and curing temperatures.

Keywords   cement; hydration; volume; modelling; MATLAB®

INTRODUCTION

Computer simulations are useful for cement scientists to observe hydration behaviour over time. This includes the dissolution of cement and gypsum and the growth of hydration products over time. While cement hydration and microstructure development is a very complex process, the advances in computing power recently have made these simulations possible. During hydration, the volume of cement and hydrates decrease and increase respectively over time and continues to do so as long as water and space are available. There is also an increase in pore space due to chemical shrinkage. HYDCEM simulates these changes in cement/binder, hydrates, water and chemical shrinkage over time using volume stoichiometries based on established material properties available in the literature.

Cement consists of four main phases, namely tri-calcium silicate ($3CaO \cdot SiO_2$, C_3S)[1], di-calcium silicate ($2CaO \cdot SiO_2$, C_2S), tri-calcium aluminate ($3CaO \cdot Al_2O_3$, C_3A) and tetra-calcium aluminate ferrite ($4CaO \cdot Al_2O_3 \cdot Fe_2O_3$, C_4AF). To perform accurate hydration simulations, it is important that the contribution from each phase is included to help identify the behaviour of existing and new cementitious materials.

HYDCEM, written in MATLAB®, determines the change in cement/binder, gypsum, magnesium and subsequent hydration products over time using built in MATLAB® functions [1-3]. HYDCEM uses a fully user-customisable MS Excel input data file to read in information on the cement being analysed including oxide composition and determines, using modified Bogue equations, the phase proportions. It also calculates the volume stoichiometries using well-established reaction molar masses in the literature. The model has built in and employs the empirical Parrot and Killoh method [4] to determine individual phase degree of hydration and uses this dissolution along with volume stoichiometries to determine the volumetric changes of the cement and of the hydration products over an user-defined time period (in hourly steps).

Over the years, a number of hydration and microstructure models have been developed that employed either the discretization, vector or cellular-automata approach using circles, spheres or discretized elements to represent cement particles. The Jennings and Johnson model [5,6] used spherical particles within a cubic volume with the reducing diameter of C_3S and increasing inner and outer C-S-H predicted as hydration continued over time. The model also determined the number of new CH particles and placed them in the pore space. In the 1990s, an integrated particle kinetics model was developed by Navi and Pignat [7-10] who simulated the hydration of spherical C_3S particles using a similar vector

---

[1] Conventional cement chemistry notation: C=CaO, S=SiO₂, A=Al₂O₃, F=Fe₂O₃, and H=H₂O.

approach as the Jennings and Johnson model [5,6]. This model used kinetic laws and relationships that simulated every particle. The HYdration, MOrphology, and STRUCtural (HYMOSTRUC) model was developed by van Breugel [11] and simulates the 3D hydration of spherical particles. Reacting particles form concentric hydrating layers around the original cement grains, which grow and intersect with each other. It employs various mass and volume balance rules to accommodate microstructural changes from the dissolution and precipitation of various phases. The HydratiCA model was developed by Bullard at NIST [12] and is based on more fundamental principles of hydration kinetics. HydratiCA makes detailed predictions of the kinetics of phase changes and microstructure development as a function of solution chemistry and temperature than other microstructure-based models of hydration.

The μic (pronounced "mike") microstructural modelling platform [13] has been written using object-oriented programming in Java and simulates the growth of millions of spherical particles representing real particle shape distributions (PSD's) to mimic hydration. The main advantage of μic is the fully customizable nature of the simulations by the user. Finally, probably the most well-known model CEMHYD3D [14], employs the discrete or pixel approach and the cellular-automata (CA) method. The microstructure is presented as a grid of discrete three-dimensional cubic elements, called volume-pixels, each representing an anhydrous or hydrate phase or pore.

To date, the development of cement hydration and microstructure models have used either the discretization or the vector approach with [15] providing a comprehensive review. This paper describes the design of HYDCEM along with examples of the customisable input files and examples of typical outputs.

HYDCEM MODEL

Model design

HYDCEM was developed to be as user friendly as possible for engineers and scientists alike. It is programmed in MATLAB® [16], which is dedicated to undertaking multiple mathematical calculations quickly. The syntax of MATLAB® is suited to engineering and scientific programming as it expresses inputs and results in matrix and vector format. By using multiple functions called from a main script allows the user to create an easy to read and edit code. While other programming languages may yield faster calculation durations, HYDCEM is capable of simulating 1,000 days of hydration (24,000 hrs) in a couple of seconds. Due to the vast amount of online documentation and help available for MATLAB® programmers, it is provides an easy to use, learn and change model for engineers and scientists.

Hydration of cement is dependent on the changes in solid volume as the hydration products continue to fill space over time. Before hydration begins, there is more cement than water if expressed by weight (the w/c ratio). However, by volume, there is more water than cement as shown in Figure 1 for a w/c ratio of 0.4 and an average cement density of 3.3g/cm^3. However, as hydration continues, the volume of water and cement decreases with a corresponding increase in hydration products and some chemical shrinkage and pore development, as predicted by [17]. Using their estimates of the change in volumetric phase fractions as a function of hydration [18], Figure 2 shows the change in volume as calculated in HYDCEM. As may be shown, there is a decrease in cement and water volume with a corresponding increase in hydration products and chemical shrinkage. These volume changes give the cement its physical properties including strength. HYDCEM predicts these changes in volume for the cement, gypsum, hydration products and water over time.
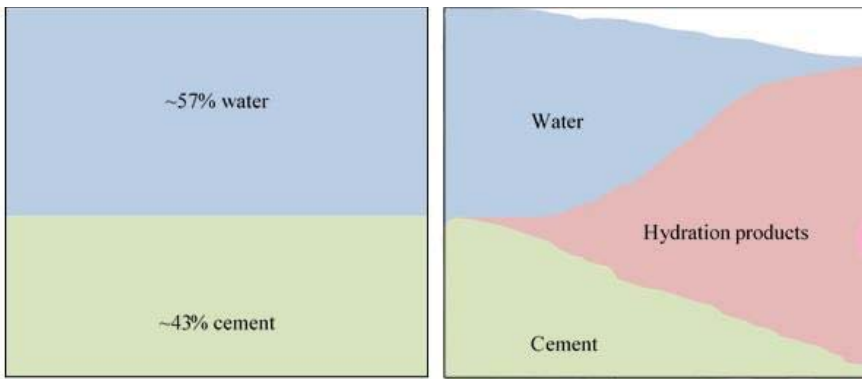

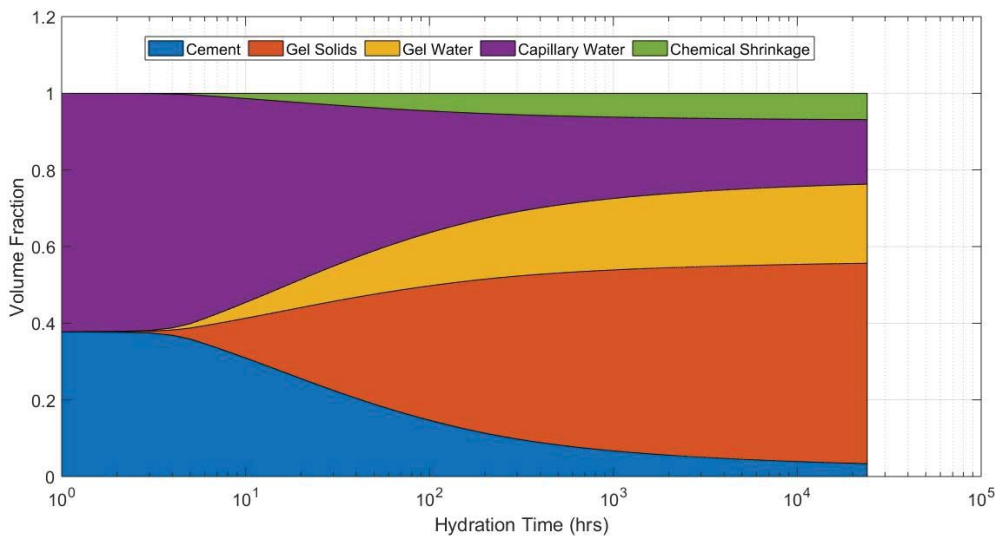Figure 1: Changes in hydration volume over time within a defined volume

Figure 2: Change in volume with ongoing hydration as predicted by [17].

Data input for HYDCEM is provided within an MS Excel spreadsheet (*input.xlsx*) with the different inputs (in numerical format) contained in individual tabs. A description of the input is provided alongside the numerical data to aid the users understanding. The input data contains information required by HYDCEM such as w/c ratio, phase heat release enthalpies, cement and hydration product densities, molar mass, molar ratio reaction and anhydrous cement oxide proportions. A suite of constants (also fully customisable) required to undertake the dissolution of the four cement phases [4] are also included in the input file. Figure 3 shows a snapshot of the input file with the densities open showing the values for the various phases and hydration products. The line of code to read these properties into the model shown below with '*densities*' representing the name of the tab within the main input file.

```
densities = xlsread('input.xlsx', 'densities');
```
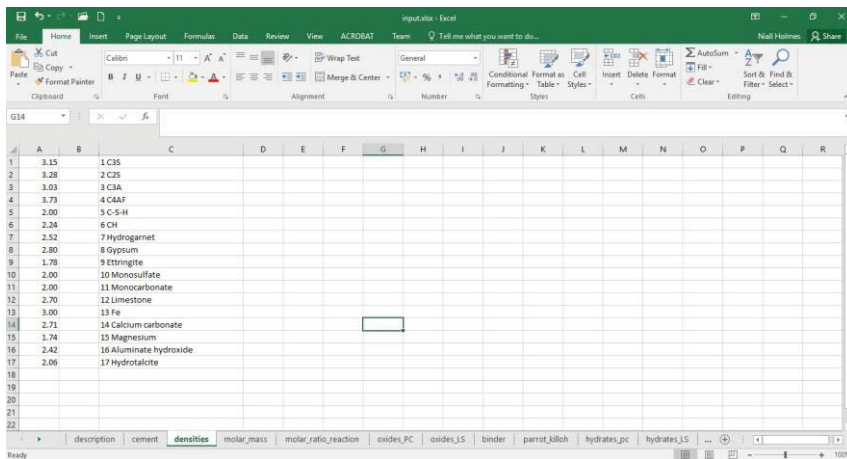

Figure 3: Snapshot of the input file (densities tab open)

The analysis/calculation flow for HYDCEM is shown in Figure 4. As may be seen, when the input data files are read into the model, the analysis follows a well-structured methodology by using multiple functions within the main HYDCEM script along with pre-allocation of single precision outputs for quicker analysis. As shown, the sequence of calculation begins with determining the chemical properties including phase proportions, volume stoichiometries and molar masses of the oxides and products. This information is then used to determine the volumes of the cement and gypsum as well as predicting the individual and overall degree of the phases and system respectively. The changing phases and gypsum volumes are used to determine the hydration products using four separate functions. Next, the heat of hydration, mortar strength and chemical shrinkage are calculated. Finally, the various graphical outputs are produced to visualise how hydration and microstructure development is progressing.

Figure 4: HYDCEM structure

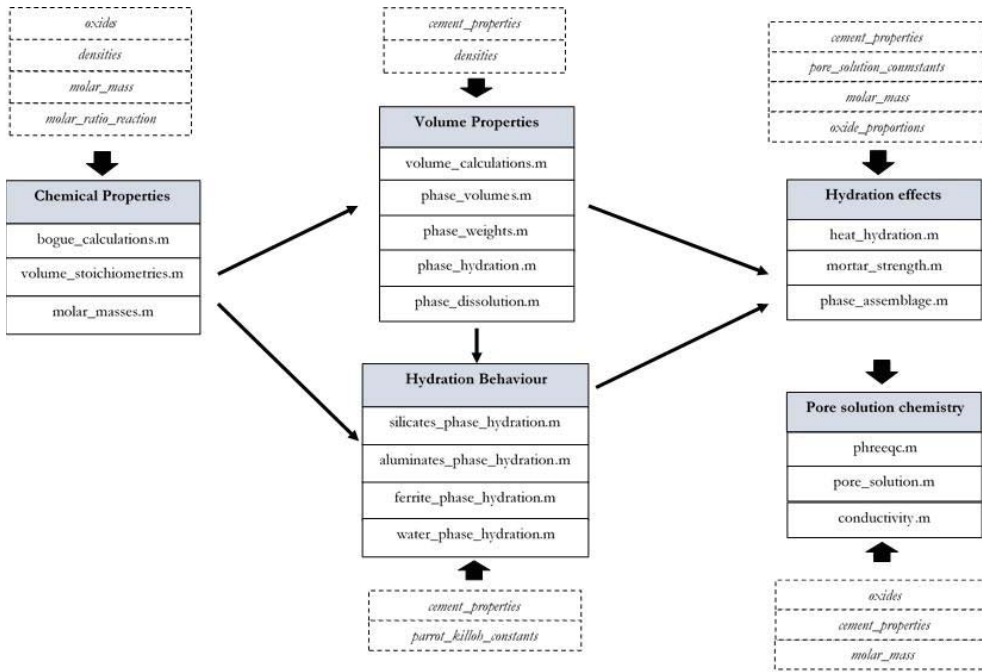The data is stored within predefined single column vectors with the number of rows equal to the number of hourly time steps. There is an expected increase in analysis time with the duration of hydration. However, as shown in Figure 5, 24,000 hourly time steps (= 1,000 days) are analysed in just over one second using an Intel® Core i7-8700 CPU desktop PC with 16Gb of RAM.
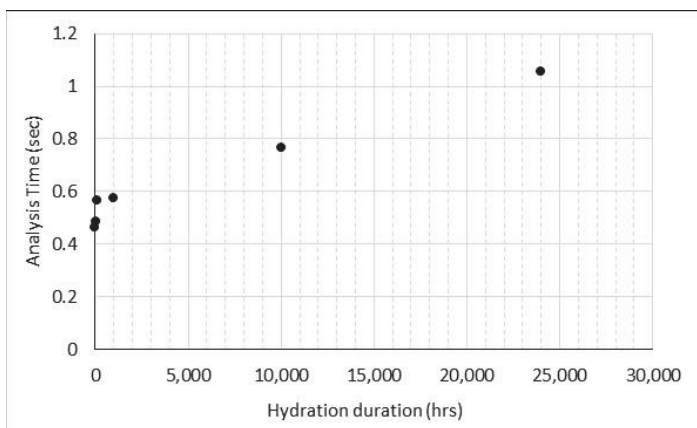

Figure 5: HYDCEM analysis times

Analysis flow

Phase proportions

Modified Bogue equations [19] are employed to determine the four phase and gypsum proportions within a function (*bogue.m*) using the oxide proportions. Modified Bogue equations have been found to yield higher C_3S and lower C_2S proportions than the standard method and gave better agreement with SEM/X-ray analysis [19]. C_3A nor C_4AF proportions did not give as good agreement but this may be due to the difficulty in distinguishing between these phases experimentally. However, as the modified Bogue equations give the best prediction of C_3S content, and due to its influence on cement hydration, this method is used in HYDCEM. Figure 6(a) and (b) show the breakdown of oxides compositions and phase proportions using the modified bogue method for the two cements described in Table 1 [20].
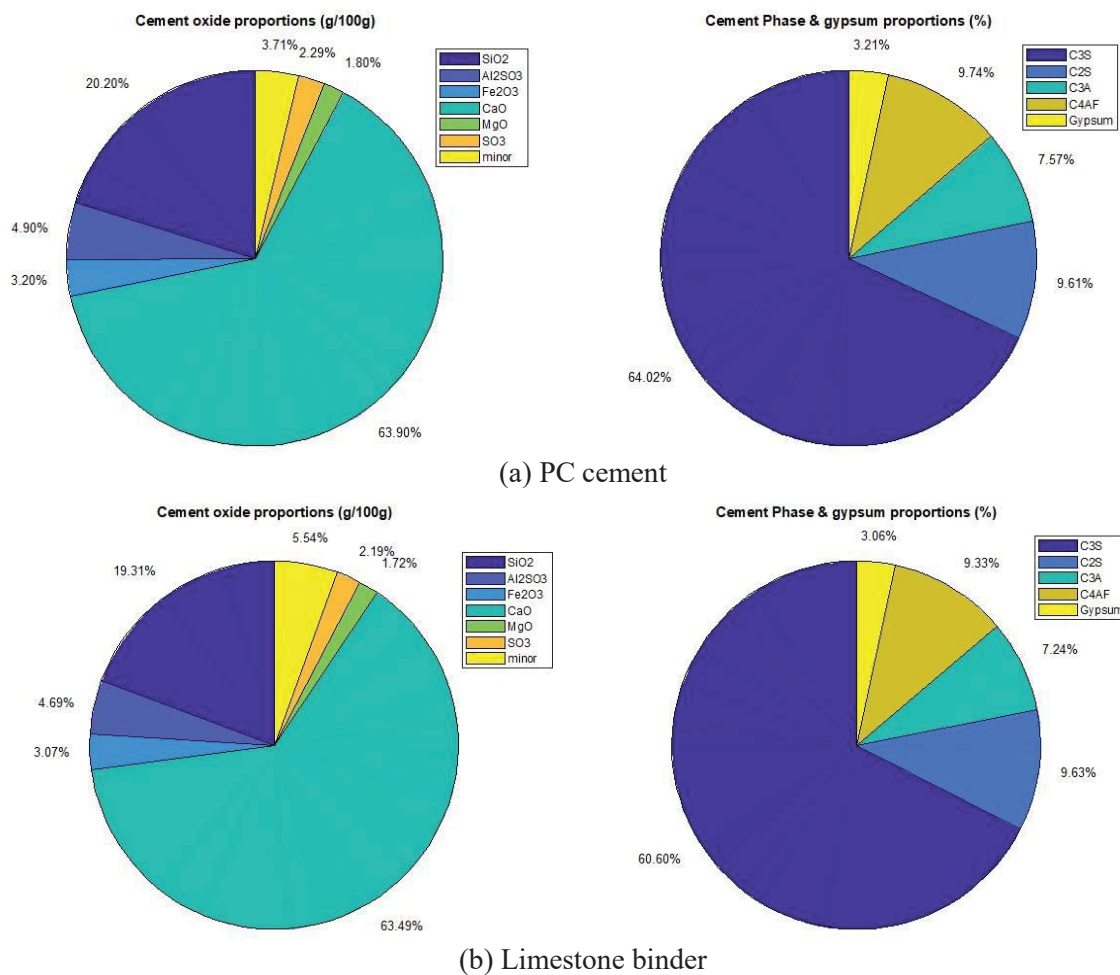

(a) PC cement

(b) Limestone binder

Figure 6: Oxide composition and phase proportions for the PC and limestone cements described in Table 1 [20]

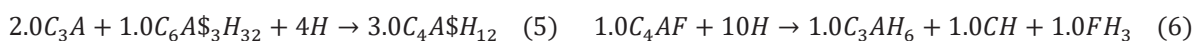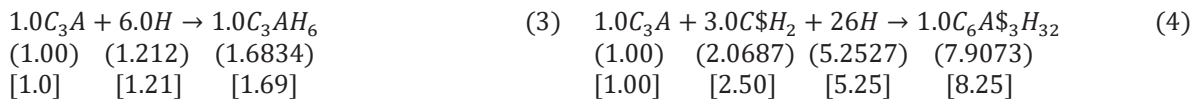Table 1: Cement chemical analysis following [from 20]

|	PC (g/100g)	Limestone (g/100g)
SiO_2	20.2	0.8
Al_2O_3	4.9	0.3
Fe_2O_3	3.2	0.3
CaO	63.9	55
MgO	1.8	1.8
Na_2O	0.42	0.01
K_2O	0.78	0.01
CaO free	0.93	0.01
CO_2	0.26	42.5
SO_3	2.29	0.05
Soluble Na_2O	0.09	0
Soluble K_2O	0.72	0
w/c ratio	0.4	
Temperature (^0C)	20	

Volume stoichiometries

The volume stoichiometries are calculated based on the molar mass reaction of the cement phase, the molar mass of the phase (C_3S, etc.) or hydration product (C-S-H, etc.) and the density, all of which are customisable by the user. The reactions of C_3A and C_4AF are dependent on the availability of gypsum and ettringite [21,22], which is coded into the model using a series of MATLAB® conditional statements. If gypsum is present, Equations (4) and (7) apply; if gypsum is consumed and ettringite is present, Equations (5) and (8) apply; finally, if both gypsum and ettringite are used up, Equations (3) and (6) apply. To aid readability, four separate MATLAB® functions for the silicates (*volume_stoichiometry_silicates.m*), aluminates (*volume_stoichiometry_aluminates.m),* ferrites (*volume_stoichiometry_ferrite),* and magnesium (*volume_stoichiometry_magnesium.m)* are called from the main script for (a) the silicates (Equations (1) & (2)), (b) aluminates (Equations (3)-(5)), (c) ferrites (Equations (6)-(8)) and (d) magnesium (Equation (9)).

The molar mass reaction for the magnesium phase and hemicarbonate [23] product are shown in Equations (9) and (10) with their calculated volume stoichiometries shown in brackets below. The volume stoichiometries used by [14] in the CEMHYD3D model are shown in square brackets below for comparison. As may be seen, there are close agreements throughout.

$1.0C_3S + 5.3H \rightarrow 1.0CSH + 1.3CH$ (1)
(1.0) (1.3173) (1.5692) (0.5933)
[1.0]   [1.34]   [1.521]   [0.61]

$1.0C_2S + 4.3H \rightarrow 1.0CSH + 0.3CH$ (2)
(1.00) (1.4752) (2.166) (0.189)
[1.0]   [1.49]   [2.077]   [0.19]

$1.0C_3A + 6.0H \rightarrow 1.0C_3AH_6$ (3)
(1.00) (1.212) (1.6834)
[1.0]   [1.21]   [1.69]

$1.0C_3A + 3.0C\$H_2 + 26H \rightarrow 1.0C_6A\$_3H_{32}$ (4)
(1.00)   (2.0687) (5.2527) (7.9073)
[1.00]   [2.50]   [5.25]   [8.25]

$2.0C_3A + 1.0C_6A\$_3H_{32} + 4H \rightarrow 3.0C_4A\$H_{12}$ (5) $1.0C_4AF + 10H \rightarrow 1.0C_3AH_6 + 1.0CH + 1.0FH_3$ (6)
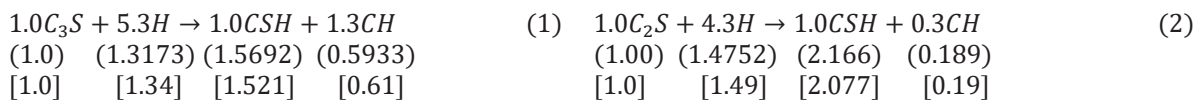
(1.00)   (3.9536) (0.4041) (5.2358)   (1.00)   (1.3828) (1.1522) (0.2539) (0.5468)
[1.00]   [4.125]   [0.404]   [5.272]   [1.0]   [1.41]   [1.17]   [0.26]   [0.545]
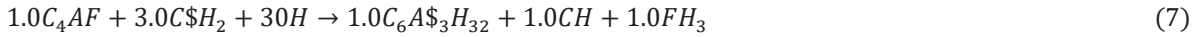
$$1.0C_4AF + 3.0C\$H_2 + 30H \rightarrow 1.0C_6A\$_3H_{32} + 1.0CH + 1.0FH_3 \tag{7}$$
(1.00)   (3.945) (4.1483)   (5.4121)   (0.2539) (05468)
[1.00]   [1.739] [4.219]   [5.739]   [0.261] [0.546]

$$2.0C_4AF + 1.0C_6A\$_3H_{32} + 12H \rightarrow 3.0C_4A\$H_{12} + 2CH + 2FH_3 \tag{8}$$
(1.00)   (2.7061) (0.8297) (3.5836) (0.2539) (0.5468)
[1.00]   [2.874]   [0.845]   [3.672]   [0.259] [0.546]

$$4MgO + 1.0Al(OH)_4 + H \rightarrow 1M_4AH_{10} \tag{9}$$
(1.00)   (0.4232) (1.9419) (1..9850)

$$C_3A + 0.5CH + 0.5CaCO_3 + 11.5H \rightarrow C_4ACO_3H_{12} \tag{10}$$
(1)   (0.185)   (0.207)   (2.323)   (2.963)

HYDCEM can also include the addition of limestone in its hydration simulations. Using the molar mass reaction for limestone [24] in Equation (11), with the calculated volume stoichiometries (*volume_stoichiometry_limestone.m*) shown in brackets below.

$$3.0C_4A\$H_{12} + 2.0C_aCO_3 + 18H \rightarrow 1.0C_6A\$_3H_{32} + 2.0C_4ACH_{11} \tag{11}$$
(1.00)   (0.079)   (0.347)   (0.757)   (0.565)

The addition of limestone is included using a separate tab within the main input file where the user can specify the oxide proportions. The binder oxide proportions to be used in the analysis when limestone is included is determined by the relative proportions and calculated within the main input file. For example, if the plain cement and limestone has a CaO oxide proportion of 65% and 55% respectively coupled with a 5% limestone percentage, the binder CaO is 64.5%.

Cement volume and weights

The volumes and weights of the four cement phases, gypsum and magnesium are determined by two separate functions (*volume_calculations.m* & *phase_volumes.m*). The results are stored within single column vectors with the number of rows equal to the number of time steps. In HYDCEM, hydration calculations are undertaken in one-hour time steps. While the duration of hydration is completely changeable by the user, the default is 24,000 hours or 1,000 days.

Cement phase dissolution calculations

The dissolution of the four cement phases in HYDCEM is simulated (*phase_dissolution.m*) using the approach presented by Parrot and Killoh [4] that uses a suite of empirical expressions to estimate the degree of hydration of each phase as a function of time. These calculations are in-built in HYDCEM

with all constants (K, N, H) and properties (activation energies, Blaine surface area, etc.) used for the procedure within [4] fully changeable by the user within the input.xlsx data file.

The dissolution of each phase is determined using Equations (12)-(14) which represent nucleation and growth, diffusion and formation of hydration shell respectively with the lowest hydration rate R_t is taken as the rate-controlling value. The degree of hydration (α) is expressed as $\alpha_t = \alpha_t - 1 + \Delta_t \cdot R_{t-1}$. The K, N and H values used for the three phases are those proposed by Lothenbach et al [20,25]. The influence of the surface area on the initial hydration are included as well as the influence of w/c ($= (1 + 3.333$ (H * w/c $- \alpha_t))^4$; for $\alpha_t > H$ * w/c.

$$R_t = \frac{K}{N}(1 - \alpha_t)(-ln(1 - \alpha_t))^{(1-N)} \tag{12}$$

$$R_t = \frac{K(1 - \alpha_t)^{\frac{2}{3}}}{1 - (1 - \alpha_t)^{\frac{1}{3}}} \tag{13}$$

$$R_t = K(1 - \alpha_t)^N \tag{14}$$

Much has been written about the appropriateness of nucleation and growth, diffusion or the formation of a hydration shell to predict cement dissolution. Dissolution theory is providing theoretical and experimental evidence to suggest the most accurate way of describing the dissolution of cement [26]. However, the Parrot and Killoh method [4] has also shown to give good comparisons with experimental results, despite being an empirical method. Until the dissolution theory is developed to a point where numerical expressions are available, HYDCEM will continue to employ the Parrot and Killoh method.

The change in individual phase volume over time is therefore determined using the product of the original phase volume and its corresponding degree of hydration. The changing phase weights (*phase_weights.m*) over time are also determined using the product of their individual degree of hydration and original weights. Figure 7 and Figure 8 show examples of HYDCEM predicted degree of hydration (using Equations 12-14) and phase weight changes over time using the PC cement properties shown in Table 1.

HYDCEM allows the user to input curing temperatures from 5 to 45^0C. As shown by [25], up to approximately 48^0C, all hydrates are stable. However, above 48^0C, monosulphate, monocarbonate and ettringite becomes unstable with the latter practically disappearing, as shown in Figure 9. HYDCEM cannot currently simulate hydration above 48^0C as the stoichiometry method employed here as described above cannot account for the behaviour shown in Figure 9. The practical applications that require such high curing temperatures ($> 45^0$C) are mostly limited to the precast concrete industry.
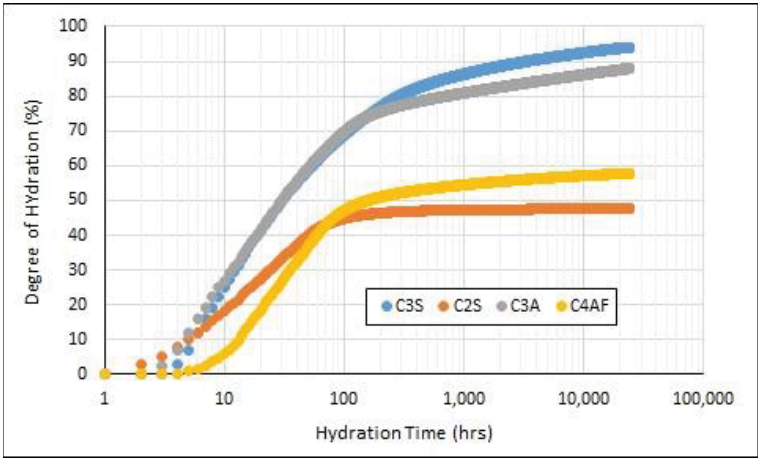
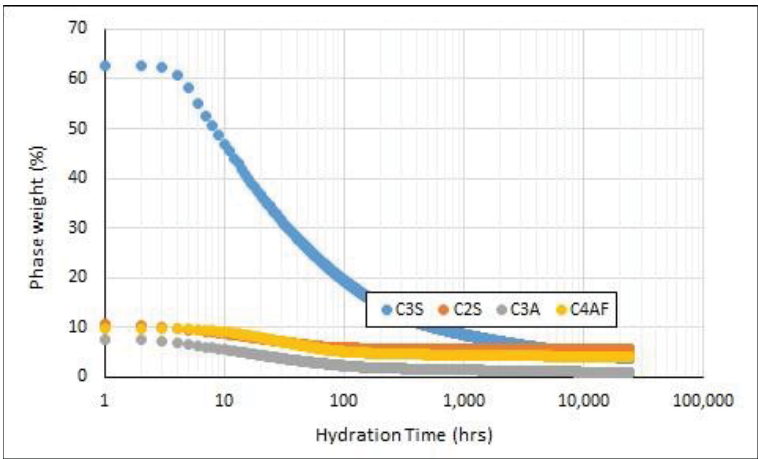Figure 7: HYDCEM degree of hydration output

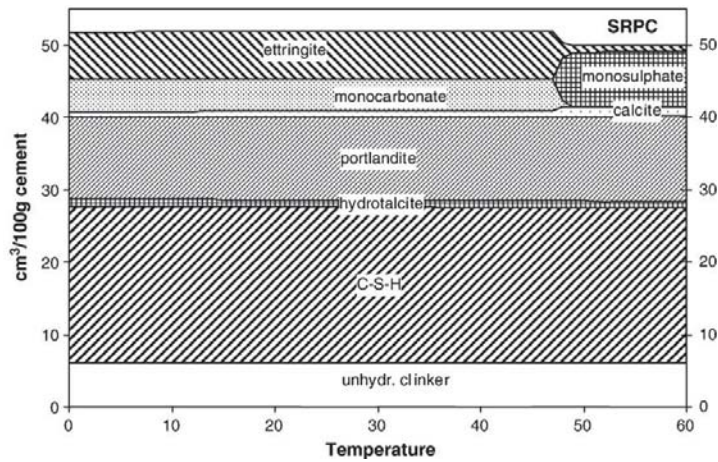Figure 8: HYDCEM change in phase weight output

Figure 9: Effect of higher temperatures on hydrates [25]

Lower curing temperatures produces a less dense C-S-H, a more even distribution of hydration products and a less course porosity [27-31]. Higher temperature cause an initially fast dissolution of the four cement phases and a more rapid precipitation of hydration products early on. This leads to higher early strength development along with a more heterogeneous distribution of hydration products in and around the clinker particles [29]. If the user does input a curing temperature lower than 5^0C or higher than 45^0C, the model will terminate.

Hydration product volumes

As hydration continues, the volume of solid products including C-S-H, calcium hydroxide (CH), ettringite, monosulphate, hydrotalcite, hydrogarnet, hemicarbonate and monocarbonate increases. These changes in volume are determined in HYDCEM via five separate functions for the silicates (*phase_hydration_silicates.m*), aluminates (*phase_hydration_aluminates.m*), ferrites (*phase_hydration_ferrite.m),* magnesium (*phase_hydration_magnesium.m*) and limestone (*limestone_hydration.m*) using the change in the four cement phases and the stoichiometries shown (in brackets) in Equations (1)-(11). This increase in hydration product as the cement phases over time is well established in the literature. Figure 10 shows some examples of this approach used by other models [13,7-9] with the reduction in C$_3$S alongside growth in inner and outer C-S-H and CH.
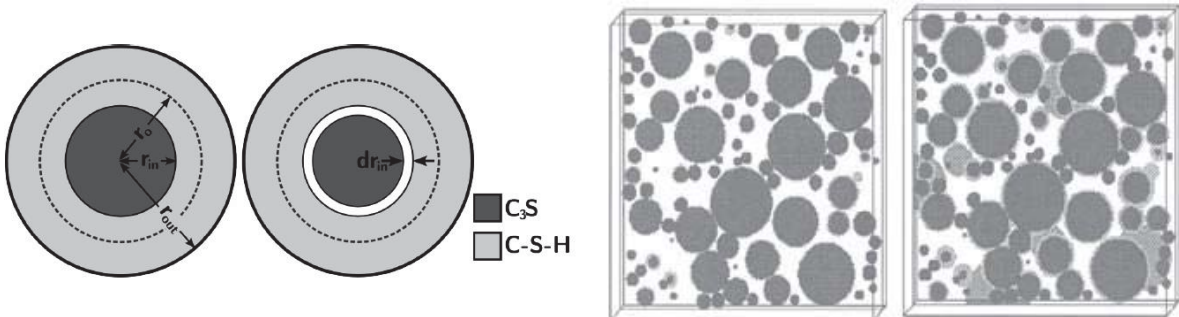

Figure 10: Increase in hydration product volume with decreasing cement phase [13,7-9]

Figure 11 shows a phase assemblage plotted in HYDCEM that demonstrates changes in cement phase, gypsum and solid volume over 1,000 days (24,000 hours) at 20^0C using the PC cement described in Table 1. HYDCEM has implemented well accepted cement hydration behaviour for the aluminates phase found in the literature. For example, the growth in monosulfate (for limestone free cements) begins after approximately three days, well after gypsum has been depleted. Also, the volume of ettringite is shown to increase until gypsum is depleted but decreases over time as it is converted to monosulphate [20]. Figure 12 shows a second HYDCEM phase assemblage for the limestone cement described in Table 1. As may be seen, the growth of monocarbonate and ettringite is shown to begin after the depletion of gypsum at one and three days respectively. It has been shown [25] that for
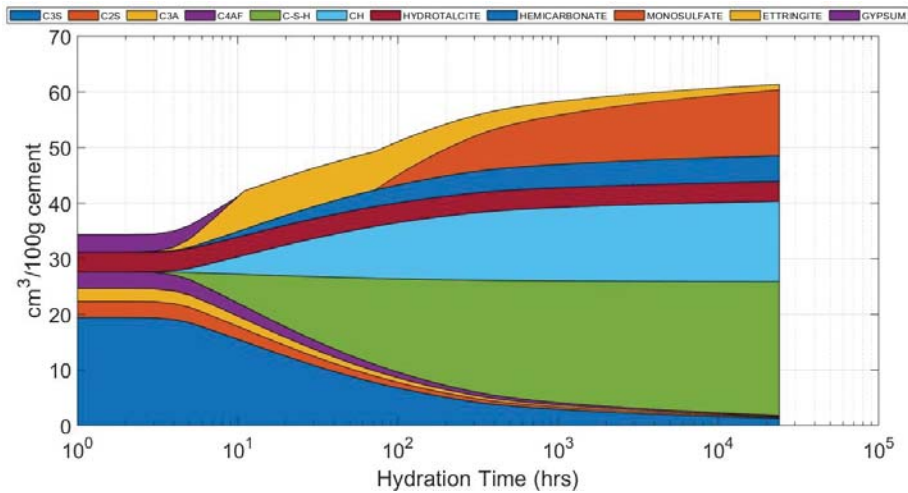
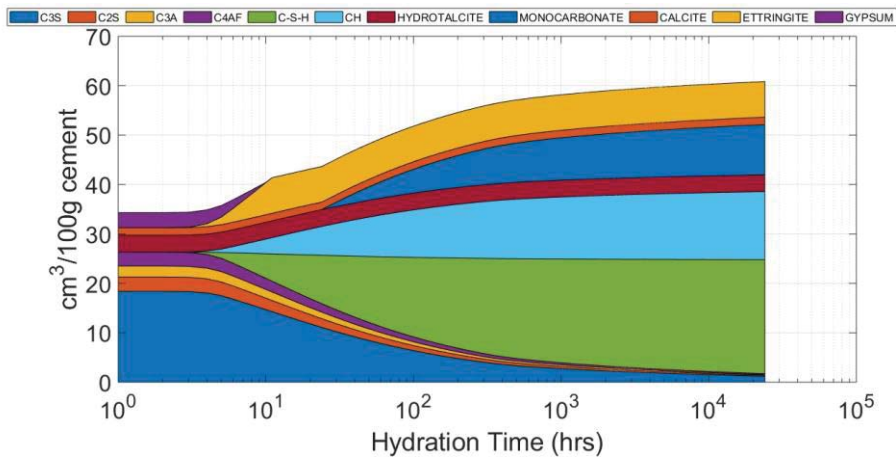Figure 11: HYDCEM Phase assemblage – PC cement

Figure 12: HYDCEM Phase assemblage – Limestone cement

limestone binders, monocarbonate forms in place of monosulfate in the limestone cement. Also, ettringite is stable in limestone binders with the growth of monocarbonate from approximately one day. These behaviours have been experimentally measured and thermodynamically modelled for plain and limestone binders by [20] and summarised in Figure 13.

Figure 14 and Figure 15 shows the growth in silicates and aluminates hydration products respectively over time. Comparing the HYDCEM predictions of aluminate changes in Figure 15 with Figure 13, it is clear that the model is mimicking the behaviours of plain and limestone cements reasonably well over time.
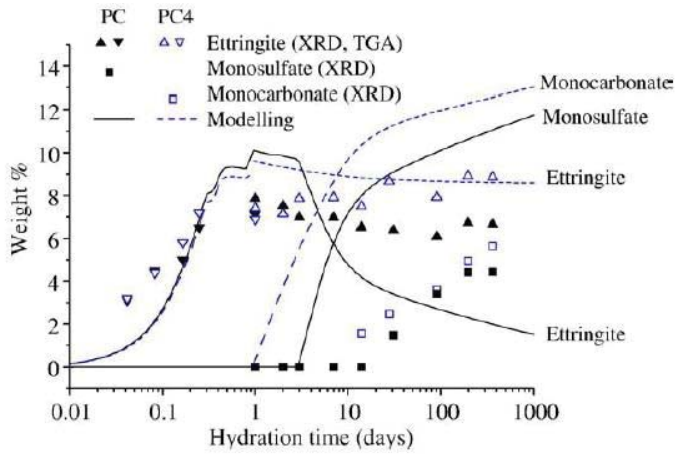
Figure 13: Results from experimentally measured and thermodynamic modelled changes during the hydration of a Portland cement with and without limestone [20]
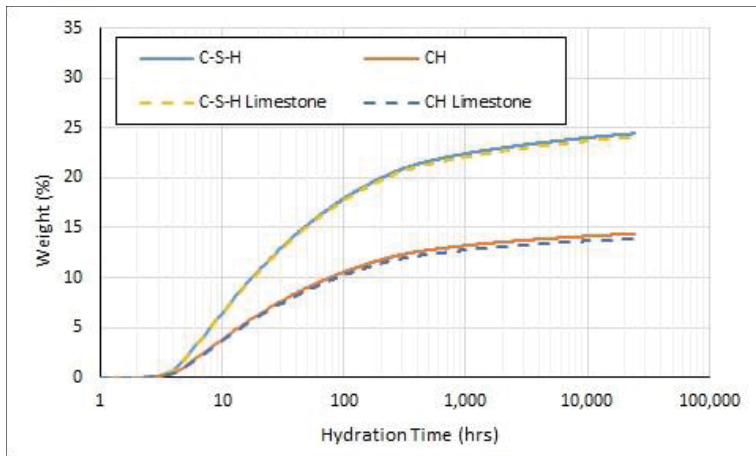

Figure 14: Silicates products of hydration with (dashed) and without (solid) limestone.
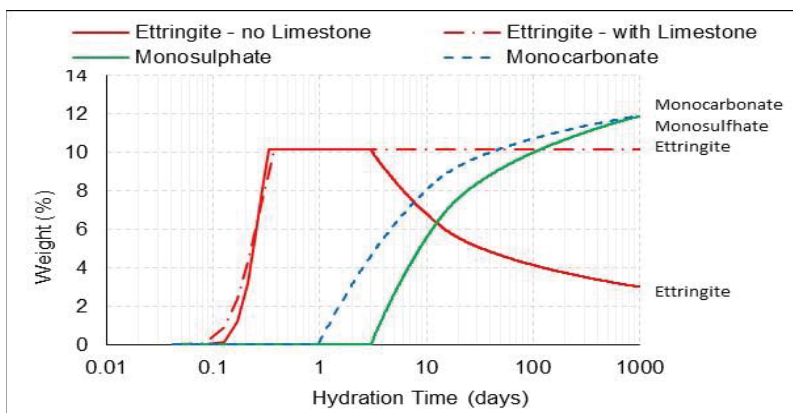

Figure 15: Aluminates products of hydration with (dashed) and without (solid) limestone.

Heat release and heat of hydration

Using published [14] enthalpies for each of the four phases (Table 2), HYDCEM provides predictions of the heat release and heat of hydration over time within a function (*heat_hydration.m*). Using these phase enthalpies and already calculated changes in phase weights at every time step, Figure 16 show the predicted heat evolutions for the PC cement described in Table 1. Previous isothermal calorimetry measurements [20] have indicated that the onset of the acceleration period begins approximately 3 hours into hydration (Figure 17a), which has been coded into HYDCEM. Figure 16(a) shows that the maximum heat flow rate is predicted to occur after nine hours, which also agrees with published experimental analysis [20] of these cements. However, while Figure 17(a) shows a slight increase in heat evolution for the limestone cements, this is not shown in the HYDCEM predictions. This is because the heat evolution is dependent on the initial phase (C_3S, C_2S, etc.) proportions. As the main oxide contents for the limestone shown in Table 1 are lower than the plain cement, the heat evolution is also lower. HYDCEM is currently unable to account for the acceleration in hydration and follow on heat evolution due to the presence of limestone which creates additional surfaces for the nucleation and growth of hydration products [30,31].

Table 2: Phase enthalpy values used in HYDCEM [14]

Phase	Enthalpy (J/g)
C_3S	517
C_2S	262
C_3A	1144
C_4AF	725
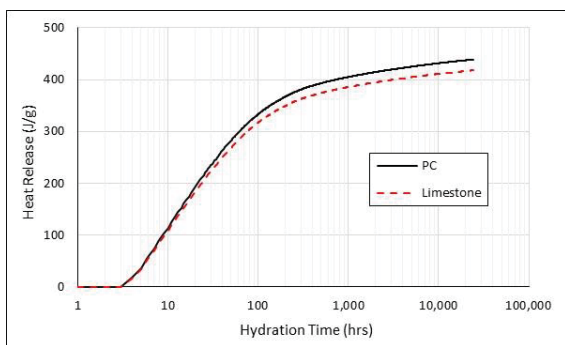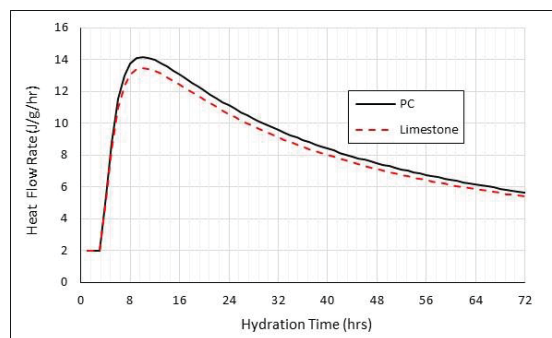
(a)   (b)

Figure 16: (a) Heat release and (b) heat flow rate prediction for PC (solid line) and limestone binder (dashed line) over time
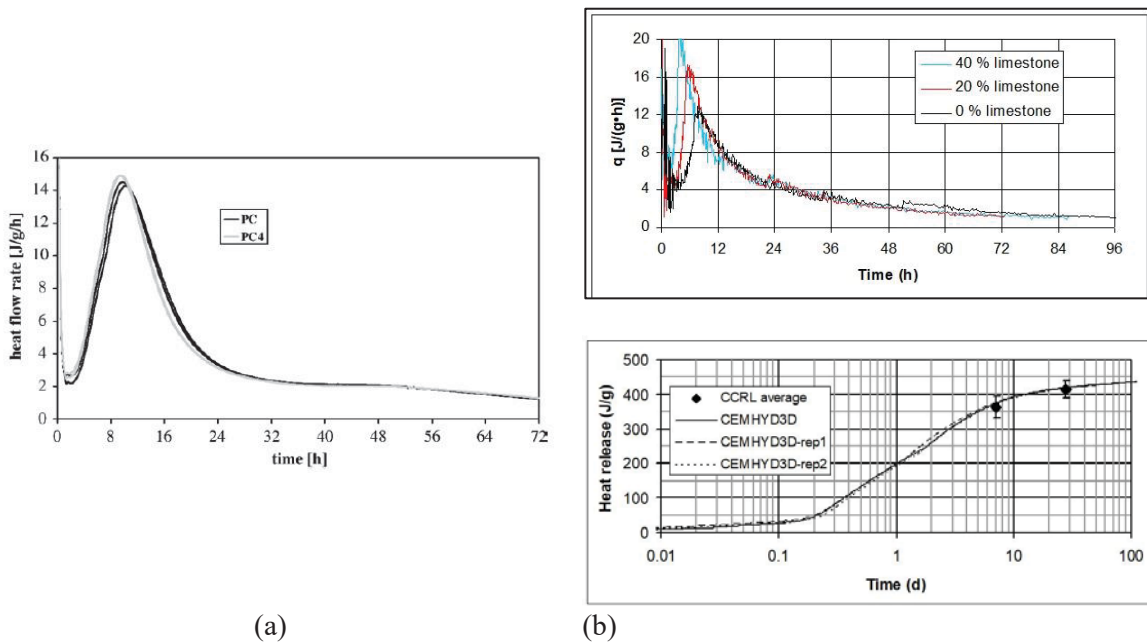
(a)   (b)

Figure 17: Published heat evolution of plain and limestone cements [20,14]

Chemical shrinkage

Chemical shrinkage during hydration arises due to the volume differences between the cement hydrating and products created and is commonly referred to as the Le Chatelier's contraction [32]. In Equation (1) for instance, the sum of the volume stoichiometries on the left (2.34) and right (2.231) hand side are different, which leads to chemical shrinkage as the hydrated products are denser than the cement and water that formed them. A function (*chemical_shrinkage.m*) in HYDCEM can predict the chemical shrinkage over time for any cement analysed. Figure 18 shows the predicted chemical shrinkage for the cement (solid line) and limestone (dashed line) as described in Table 1. As may be seen, the chemical shrinkage for the limestone binder is slightly less than the plain cement. This is contrary to [32] who found the presence of limestone accelerated chemical shrinkage due to the additional surface area. Figure 19 shows measured chemical shrinkage from [33] for various cements and w/c ratios. There is reasonably good agreement between Figure 18 and Figure 19.

Estimation of mortar compressive strength

Using Powers' gel-space ratio principal in Equation (15) [34-36] where X is the gel-space ratio and α is the overall degree of hydration, HYDCEM can give a prediction of the mortar compressive strength development over time. The α term in Equation 15 is calculated using Equation 16 where α^p is the individual phase degree of hydration and $prop^p$ is the proportion (%) of C_3S, C_2S, etc.

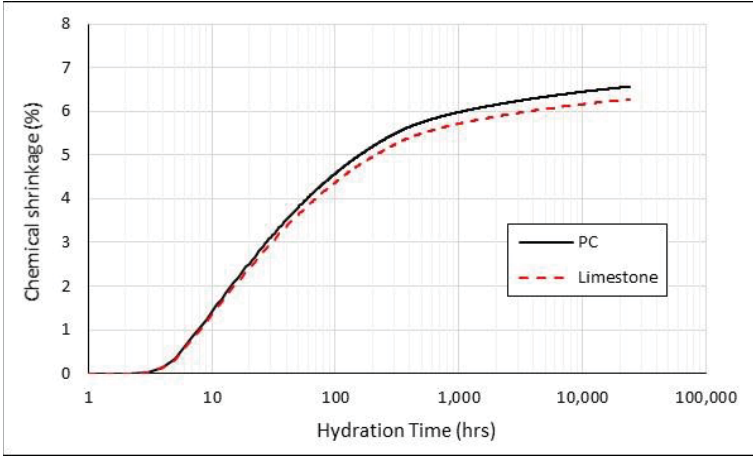Figure 18: HYDCEM predicted chemical shrinkage. Solid line = PC; dashed line = Limestone

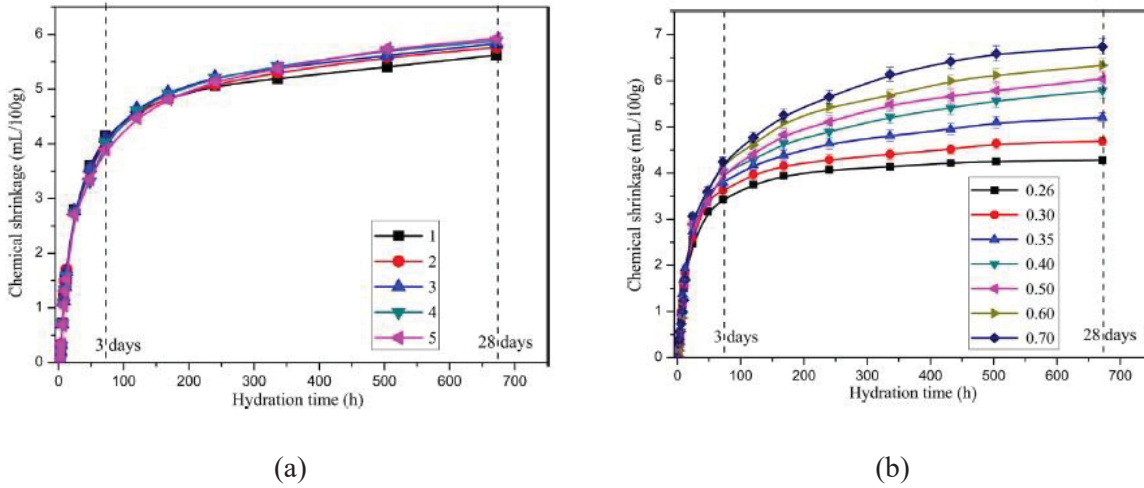(a)   (b)

Figure 19: Measured chemical shrinkage for various cements and w/c ratio from the literature [33]

Previous work by [34] has shown that the compressive strength of ASTM C109 mortar cubes [37] over time can be predicted using Equation 17, where X is the gel-space ratio (Equation 14), σ_A is the intrinsic strength of the cement and n is a constant that, depending on the cement, ranges between 2.6 and 3.0. For C_3A Bogue contents below 7%, the value of σ_A should be lower [40]. Bentz [34] used intrinsic strength values of 129 and 99MPa for NIST Cements 115 and 116 respectively with a w/c ratio of 0.485 that provided good correlations between measured and predicted, as shown in Figure 20. The values for σ_A and n are provided in the input file and changeable by the user.

$$X = \frac{0.68\alpha}{0.32\alpha + w/c} \tag{15}$$

$$\alpha = \frac{prop^{C3S}\alpha^{C3S} + prop^{C2S}\alpha^{C2S} + prop^{C3A}\alpha^{C3A} + prop^{C4AF}\alpha^{C4AF}}{prop^{C3S} + prop^{C2S} + prop^{C3A} + prop^{C4AF}} \tag{16}$$

$$\sigma_c(t) = \sigma_A X(t)^n \tag{17}$$

An example of the HYDCEM predicted compressive strengths using the above approach using for the plain cement in Table 1 is shown in Figure 21. An intrinsic strength and n value of 83.55MPa and 2.6 respectively were used. Work is underway to cast, measure and predict compressive strengths using ASTM C109 [37] mortar cubes where intrinsic strength and n values can be developed for various w/c ratios and curing temperatures.
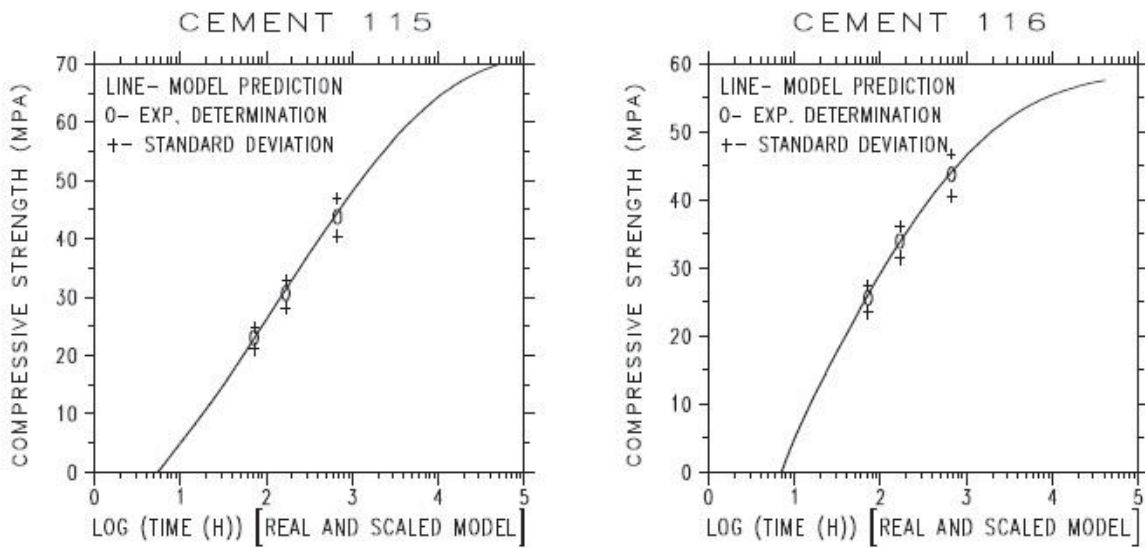

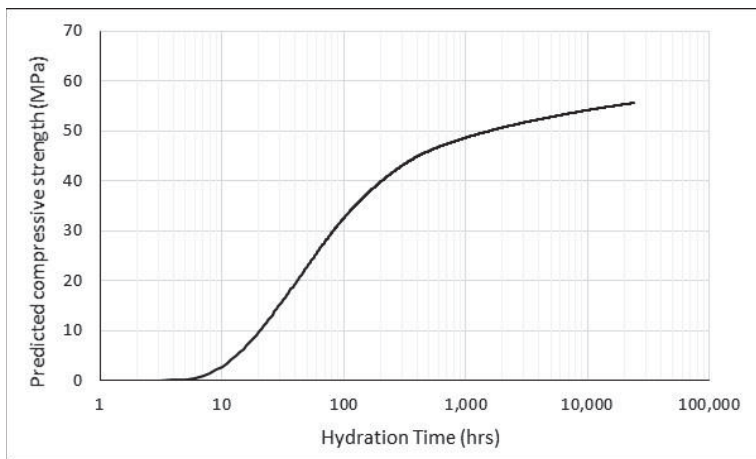Figure 20: Predicted and measured compressive strengths for NIST Cements 115 and 116 [34]

Figure 21: Predicted mortar compressive strength

CONCLUSIONS

A new model, HYDCEM, has been presented that simulates the volume changes in cement phase and hydration products over time. The model, written in MATLAB®, is capable of simulating over 1,000 days of hydration in a few seconds. It has been designed to be as user-friendly as possible with easy to read, understand and change input data via an EXCEL spreadsheet using multiple tabs. HYDCEM incorporates established hydration behaviour in the literature by using MATLAB® statement operators. These have provided good predictions compared with published experimental results of phase dissolution, hydration product volume growth and heat release. Ongoing work to couple HYDCEM with the PHREEQC thermodynamic model will provide a long-term/equilibrated prediction of the pore water chemistry.

HYDCEM is intended to complement more sophisticated thermodynamic models to allow engineers and cement scientists to assess existing and new cements using its chemical/oxide proportions, w/c ratio and curing temperature. Most data required by HYDCEM to run an analysis is available in the literature, for instance phase and product density, molar masses, enthalpies, molar ratio of reaction and parameters for the Parrot & Killoh methodology to predict phase dissolution.

HYDCEM currently simulates the hydration of plain (PC) and limestone cements. Work is ongoing to model the effects of supplementary cementitious materials additions including GGBS and fly ash.

ACKNOWLEDGEMENTS

REFERENCES

[1] Holmes, N., Griffin, A., Enright, B. & Kelliher, D (2018) Introducing a new cement hydration and microstructure model, Civil Engineering Research in Ireland Conference, pp. 202-207, August, University College Dublin, Ireland.

[2] Holmes, N., Kelliher, D. & Tyrer, M. (2019) HYDCEM: A new cement hydration model, ICSBM 2019 2nd International Conference of Sustainable Building Materials, pp. 66-74, 12-15 August, Eindhoven The Netherlands.

[3] Holmes, N., Kelliher, D. & Tyrer, M. (2019) Modelling the addition of limestone in cement using HYDCEM, 39th Cement and Concrete Science Conference, pp. 23-27, 9-10th September 2019, University of Bath, UK.

[4] L.J. Parrot, D.C. Killoh, Prediction of cement hydration, Br. Ceram. Proc. 35 (1984) 41–53.

[5] H.M. Jennings, S.K. Johnson, Simulation of microstructure development during the hydration of a cement compound, Journal of the American Ceramic Society 69 (1986) 790–795.

[6] S.K. Johnson, H.M. Jennings, Computer simulated hydration of a cement model, Proceedings of the 10th CIB congress, International Council for Building Research, Studies, and Documentation, Washington D.C., U.S.A., 1986, pp. 2086–2095.

[7] P. Navi, C. Pignat, Simulation of cement hydration and the connectivity of the capillary pore space, Advanced Cement Based Materials 4 (1996) 58–67.

[8] P. Navi, C. Pignat, Three-dimensional characterization of the pore structure of a simulated cement paste, Cement and Concrete Research 29 (1999) 507–514.

[9] P. Navi, C. Pignat, Effects of cement size distribution on capillary pore structure of the simulated cement paste, Computational Materials Science 16 (1999) 285–293.

[10] C. Pignat, P. Navi, K. Scrivener, Simulation of cement paste microstructure hydration, pore space characterization and permeability determination, Materials and Structures 38 (2005) 459–466.

[11] K. van Breugel, Numerical simulation of hydration and microstructural development in hardening cement-based materials (I): Theory, Cement and Concrete Research 25 (1995) 319–331.

[12] J.W. Bullard, A three-dimensional microstructural model of reactions and transport in aqueous mineral systems, Modell. Simul. Mater. Sci. Eng. 15 (2007) 711–738.

[13] Bishnoi, S and Scrivener, K.L (2009) µic: A new platform for modelling the hydration of cements, Cement and Concrete Research 39, pp. 266–274.

[14] Bentz D.P. CEMHYD3D: A three-dimensional cement hydration and microstructure development modelling package. Version 2.0. NISTIR 6485, US Department of Commerce, April 2000.

[15] J.J. Thomas, J.J. Biernacki, J.W. Bullard, S. Bishnoi, J.S. Dolado, G.W. Scherer, A. Luttge, Modeling and simulation of cement hydration kinetics and microstructure development, Cement and Concrete Research 41 (2011) 1257–1278

[16] Mathworks https://uk.mathworks.com/products/matlab.html

[17] Powers, T.C., and Brownyard, T.L., Studies of the Physical Properties of Hardened Portland Cement Paste, ACI Journal, Proceedings V. 43, Oct. 1946 to Apr. 1947 (published in multiple parts); also published as PCA Bulletin 22, Research Laboratories of the Portland Cement Association, Chicago, IL, 1948.

[18] Bentz DP, Irassar EF, Bucher BE, Weiss WJ. Limestone fillers conserve cement; Part 1: an analysis based on Powers' model. Concr Int. 2009;31:41-46.

[19] ASTM C150-09, standard specification for portland cement. Annual Book of ASTM Standards, ASTM International, West Conshocken, PA, 4.

[20] Lothenbach, B., Le Saout, G., Gallucci, E. and Scrivener, K. (2008) Influence of limestone on the hydration of Portland cements, Cement and Concrete Research 38 pp. 848–860.

[21] Bentz, D.P., Coveney, P.V., Garboczi, E.J., Kleyn, M.F. and Stutzman, P.E. (1994). Cellular automaton simulations of cement hydration and microstructure development. Modelling and Simulation in Materials Science and Engineering, 2(4), pp.783-808.

[22] Merzouki, T., Bouasker, M., Khalifa, N.E.H. and Mounanga, P. (2013). Contribution to the modelling of hydration and chemical shrinkage of slag-blended cement at early age. Construction and Building Materials, 44, pp.368-380.

[23] Brouwers, H.J.H. & B. Fisher, H. (2003). Chemical Reactions in hydrated Ordinary Portland Cement based on the work by Powers and Brownyard. IEEE Transactions on Magnetics - IEEE TRANS MAGN.

[24] Mohamed, A.R., Elsalamawy, M and Ragab, M (2015) Modelling the influence of limestone addition on cement hydration, Alexandria Engineering Journal 54, pp. 1–5.

[25] Lothenbach, B., Winnefeld, F., Alder, C., Wieland, E., and Lunk, P. (2007) Effect of temperature on the pore solution, microstructure and hydration products of Portland cement pastes, Cement and Concrete Research 37 (4) pp. 483–491.

[26] Juilland, P., Gallucci, E., Flatt, R and Scrivener, K (2010) Dissolution theory applied to the induction period in alite hydration, Cement and Concrete Research 40 831–844

[27] Lothenbach, B. Thermodynamic modelling of the effect of temperature on the hydration of Portland cement, International RILEM Symposium on Concrete Modelling – CONMOD 2008, 26-28 May, Delft, The Netherlands.

[28] Kjellsen, K.O., Detwiler, R.J, (1992) Reaction-kinetics of Portand-cement mortors hydrated at different temperatures, Cement & Concrete Research 22 (1), pp. 112-120.

[29] Escalante-Garcia, J.I., Sharp, J.H. (1998) Effect of temperature on the hydration of the main clinker phases in Portland cements: Part I, neat cements, Cement & Concrete Research 28 (9), pp. 1245-1257.

[30] Komonen, J., Penttala, V. (2003) Effects of high temperatures on the pore structure and strength of plain and polypropylene fiber reinforced cement pastes, Fire Technol 39 (1), pp. 23-34.

[31] Thomas, JJ., Rothstein, D., Jennings, H.M., Christensen, B.J. (2003), Effect of hydration temperatures on the solubility behaviour of Ca-, S-, Al- and Al- and Si- bearing solid phases in Portland cement pastes, Cement & Concrete Research 33 (12), pp. 2037-2047.

[32] Bouasker, M., Mounanga, P., Turcry, P., Loukili, A. and Khelidj, A. (2008) Chemical shrinkage of cement pastes and mortars at very early age: Effect of limestone filler and granular inclusions, Cement and Concrete Composites, Vol. 30, pp. 13–22.

[33] Tongsheng Zhang, Peng Gao, Ruifeng Luo, Yiqun Guo, Jiangxiong Wei, Qijun Yu (2013) Measurement of chemical shrinkage of cement paste: Comparison study of ASTM C 1608 and an improved method, Construction and Building Materials 48, pp. 662–669

[34] Bentz, D.P., "A Three-Dimensional Cement Hydration and Microstructure Program. I. Hydration Rate, Heat of Hydration, and Chemical Shrinkage," NISTIR 5756, U.S. Department of Commerce, November 1995 (available from National Technical Information Service).

[35] Bentz, D.P., "Three-Dimensional Computer Simulation of Cement Hydration and Microstructure Development," J Amer Ceram Soc, Vol. 80 (1), 3-21 (1997).

[36] Powers, T.C., "Physical Properties of Cement Paste," in Proceedings of the 4th International Symposium on the Chemistry of Cement, Washington, D.C., Vol. 2, Paper V-1, 577-613 (1962).

[37] Annual Book of ASTM Standards, Vol. 04.01. Cement; Lime; Gypsum (ASTM, Philadelphia, PA, 1992).